

See discussions, stats, and author profiles for this publication at: <https://www.researchgate.net/publication/231373798>

Modeling Transient Permeation of Binary Mixtures through Zeolite Membranes

ARTICLE *in* INDUSTRIAL & ENGINEERING CHEMISTRY RESEARCH · JULY 2006

Impact Factor: 2.59 · DOI: 10.1021/ie060166u

CITATIONS

13

READS

30

4 AUTHORS, INCLUDING:



Tracy Q. Gardner

Colorado School of Mines

17 PUBLICATIONS 303 CITATIONS

SEE PROFILE

Modeling Transient Permeation of Binary Mixtures through Zeolite Membranes

Janna G. Martinek,[†] Tracy Q. Gardner,[‡] Richard D. Noble,[†] and John L. Falconer^{*,†}

Department of Chemical and Biological Engineering, University of Colorado, Boulder, Colorado 80309-0424, and Department of Chemical Engineering, Colorado School of Mines, Golden, Colorado 80401

Transient permeation of binary mixtures through zeolite membranes was modeled by Maxwell–Stefan diffusion and extended Langmuir adsorption. The permeate response of the faster-diffusing component overshoots its steady-state permeance, even when adsorption properties of the two components are identical. For zero permeate pressure and negligible support resistance, the adsorption equilibrium constants only affect the transient response by determining feed occupancies. Both higher permeate pressures and more support resistance decrease the overshoot in the permeate response of the faster-diffusing component. In some cases, molecules transport through the membranes against their concentration gradient under transient conditions because of the influence of slower-diffusing molecules. At steady-state, slower-diffusing molecules can cause faster-diffusing molecules to transport against their concentration gradient for high permeate pressures or substantial support resistance.

Introduction

Zeolites are inorganic crystalline structures with uniform-sized pores of molecular dimensions. Zeolite membranes are continuous polycrystalline films of zeolites grown on porous supports, which provide mechanical stability, and these membranes are chemically and thermally stable. The molecular-size pores and the adsorption properties give zeolite membranes the potential to carry out many industrially useful separations with high selectivities and low energy demands. Separations using zeolite membranes are the result of a combination of differences in diffusivities and preferential adsorption, and separations can favor either the more mobile or the more strongly adsorbing component. Surface diffusion is the dominant transport mechanism for zeolite membranes; molecules adsorb on the feed-side surface, diffuse through the pores by jumping from site to site in the direction of decreasing chemical potential, and desorb from the zeolite on the permeate side.¹ Flow through the porous support is a combination of bulk diffusion, Knudsen diffusion, and viscous flow.²

Surface diffusion in zeolites has been modeled by the generalized Maxwell–Stefan equations,^{2–9} because Fickian diffusion with a concentration-independent diffusion coefficient fails to qualitatively describe some transport behavior observed in zeolites.^{6,10} Krishna and co-workers modeled permeation of single-component and binary mixtures using both single- and dual-site Langmuir isotherms.^{3–6,11} Extended Langmuir isotherms were used for the two-component system. The extended Langmuir isotherm is a good representation when the saturation loadings of the two components are the same or similar. When the saturation loadings differ significantly, however, extended Langmuir isotherms do not predict observed behavior, particularly at high occupancies, where the component with higher saturation loading can dominate adsorption.^{5,12–14}

Transient response measurements for zeolite membranes have the potential to provide much more information than can be obtained from steady-state measurements, because the adsorption and diffusion steps can be distinguished. Membranes with the same steady-state flux, for example, can have quite different

transport pathways and, thus, different transient behavior. Thus, transient measurements are of particular value in understanding diffusion in zeolite membranes and how one molecule affects diffusion of a second molecule. Transient measurement can be used to characterize membranes nondestructively, measure adsorption isotherms, and study diffusion in zeolites.^{15–20} Although the emphasis here is on zeolite membranes, similar transient behavior would be expected for other nanoporous membranes.

Gardner and co-workers modeled transient behavior for single-component transport through zeolite membranes for both single-site and dual-site Langmuir isotherms.^{15–18} Their model was used to determine adsorption isotherms for single components in zeolite membranes from transient permeate responses. Helium was used as a diluent on the feed side and as a sweep gas on the permeate side because it adsorbs weakly in zeolites. Adsorption isotherms were determined from a mass balance.

The current study examines transient permeation of binary mixtures through zeolite membranes in order to determine the type of behavior expected for transient experiments. The objectives are to determine the following for mixtures: (1) the role of adsorption equilibrium constants in transient responses, (2) how differences in diffusivities affect transient responses, (3) how to analyze transient behavior at high occupancies, and (4) the influence of the support on transient responses. Unlike single-component transients, the permeate responses of the faster-diffusing component overshoot their steady-state permeances, and the transient profiles for the fractional occupancy of the faster-diffusing component develop qualitatively differently than those of a single component, even when the adsorption strengths of the two components are the same. Analysis was carried out for a range of conditions.

Modeling

Maxwell–Stefan Model. The transient Maxwell–Stefan (M–S) model is a system of coupled, partial differential equations that were solved by finite difference methods. The generalized M–S equations²

$$-\rho \frac{\partial_i}{RT} \nabla \mu_i = \sum_{j=1}^n \frac{q_j J_i - q_i J_j}{q_i^{\text{sat}} q_j^{\text{sat}} \Phi_{ij}} + \frac{J_i}{q_i^{\text{sat}} \Phi_i} \quad i = 1, 2, \dots, n \quad (1)$$

* Corresponding author. E-mail: john.falconer@colorado.edu.
Tel.: (303) 492-8005. Fax: (303) 492-4341.

[†] University of Colorado.

[‡] Colorado School of Mines.

balance the chemical potential gradient of species i , which is the driving force for species i (left-hand side of eq 1), with the friction exerted by species j on the motion of species i (first term on the right-hand side) and the friction between species i and the adsorbent surface (second term on right-hand side). In these equations, θ_i is the fractional surface occupancy of species i , q_i is the loading of component i , q_i^{sat} is the saturation loading of component i , J_i is the flux of species i , Θ_i is the single-component M–S diffusivity of species i , Θ_{ij} is the M–S diffusivity representing interchange between species i and j , and ρ is the density of the zeolite. The single-component M–S diffusivities were assumed to be independent of concentration. This assumption may be reasonable for some systems,^{21,22} but M–S diffusivities can depend on concentration, even at low loadings.^{21–25}

The chemical potential gradient can be expressed in terms of the fractional occupancy gradient via thermodynamic correction factors Γ_{ij} defined by²

$$\frac{\theta_i}{RT} \nabla \mu_i = \sum_{j=1}^n \Gamma_{ij} \nabla \theta_j \quad i, j = 1, 2, \dots, n \quad (2)$$

$$\Gamma_{ij} = \theta_i \frac{\partial \ln p_i}{\partial \theta_j} \quad i, j = 1, 2, \dots, n \quad (3)$$

where p_i is the partial pressure of component i in the bulk fluid and the equilibrium relationship between p_i and θ_i defines the partial derivatives in eq 3. For a single-site, extended Langmuir isotherm, the thermodynamic correction factors for a binary mixture are

$$\begin{aligned} \Gamma_{11} &= \frac{1 - \theta_2}{1 - \theta_1 - \theta_2} & \Gamma_{12} &= \frac{\theta_1}{1 - \theta_1 - \theta_2} \\ \Gamma_{21} &= \frac{\theta_2}{1 - \theta_1 - \theta_2} & \Gamma_{22} &= \frac{1 - \theta_1}{1 - \theta_1 - \theta_2} \end{aligned} \quad (4)$$

Combining eqs 1 and 2, assuming that $\Theta_{12} = \Theta_{21}$, and solving for the fluxes yields³

$$J_1 = -\rho q_1^{\text{sat}} \Theta_1 \times \frac{\left[\Gamma_{11} + \theta_1 \frac{\Theta_2}{\Theta_{12}} (\Gamma_{11} + \Gamma_{21}) \right] \nabla \theta_1 + \left[\Gamma_{12} + \theta_1 \frac{\Theta_2}{\Theta_{12}} (\Gamma_{12} + \Gamma_{22}) \right] \nabla \theta_2}{1 + \theta_2 \frac{\Theta_1}{\Theta_{12}} + \theta_1 \frac{\Theta_2}{\Theta_{12}}} \quad (5)$$

$$J_2 = -\rho q_2^{\text{sat}} \Theta_2 \times \frac{\left[\Gamma_{22} + \theta_2 \frac{\Theta_1}{\Theta_{12}} (\Gamma_{22} + \Gamma_{12}) \right] \nabla \theta_2 + \left[\Gamma_{21} + \theta_2 \frac{\Theta_1}{\Theta_{12}} (\Gamma_{21} + \Gamma_{11}) \right] \nabla \theta_1}{1 + \theta_1 \frac{\Theta_2}{\Theta_{12}} + \theta_2 \frac{\Theta_1}{\Theta_{12}}} \quad (6)$$

The interchange coefficient Θ_{ij} is calculated as a logarithmic average of the single-component M–S diffusivities:⁴

$$\Theta_{12} = \Theta_1^{\theta_1/(\theta_1+\theta_2)} \Theta_2^{\theta_2/(\theta_1+\theta_2)} \quad (7)$$

When the saturation loadings of the two components differ, and the single-component M–S diffusivities are occupancy dependent,^{17,26} Skouidas et al. suggest a modified formula in which $\Theta_{12} \neq \Theta_{21}$,²⁶ but the saturation loadings were assumed to be

the same in this study. This modified formula quantitatively agreed with molecular dynamics simulations for binary mixtures of light alkanes and CF₄ in MFI, FAU, and LTA type zeolites.^{25–27} Equation 7 may not be appropriate when the two components exhibit attractive interactions in the zeolite pores or when the zeolite is not homogeneous.

The transient surface occupancies are described by⁴

$$\frac{\partial \theta_i}{\partial t} = -\frac{1}{\rho q_i^{\text{sat}}} \frac{\partial J_i}{\partial z} \quad (8)$$

When the membrane is initially empty, the boundary and initial conditions are

$$\theta_i(0, t) = \frac{b p_{i,\text{feed}}}{1 + b_1 p_{1,\text{feed}} + b_2 p_{2,\text{feed}}} \quad (9)$$

$$\begin{aligned} \theta_i(\delta, t) &= \frac{b p_{i,\text{perm}}}{1 + b_1 p_{1,\text{perm}} + b_2 p_{2,\text{perm}}} \\ \theta_i(z, 0) &= 0 \\ J_i(z, 0) &= 0 \end{aligned} \quad (10)$$

When the membrane initially contains one component at steady state, analytical solutions for its fractional occupancy profile and flux (eqs 11 and 12)¹⁵ are used along with the boundary conditions in eq 9.

$$\begin{aligned} \theta_1(z, 0) &= 1 - \left(\frac{1}{1 + bp_{\text{feed}}} \right) \left(\frac{1 + bp_{\text{feed}}}{1 + bp_{\text{perm}}} \right)^{z/\delta} \\ J_1(z, 0) &= \frac{\rho q_i^{\text{sat}} \Theta}{\delta} \ln \left(\frac{1 + bp_{\text{feed}}}{1 + bp_{\text{perm}}} \right) \end{aligned} \quad (11)$$

$$\begin{aligned} \theta_2(z, 0) &= 0 \\ J_2(z, 0) &= 0 \end{aligned} \quad (12)$$

Support Resistance. Bulk diffusion, Knudsen diffusion, and viscous flow are included in the transport model for the support. The contributions from bulk and Knudsen diffusion are²

$$-\frac{1}{RT} \nabla p_i = \sum_{\substack{j=1 \\ j \neq i}}^n \frac{x_j J_{\text{md},i} - x_i J_{\text{md},j}}{\epsilon D_{ij}} + \frac{J_{\text{md},i}}{D_{\text{Kn},i}} \quad i = 1, 2, \dots, n \quad (13)$$

in which the force contributing to the motion of species i is balanced with the friction due to interactions with species j and the pore walls. In these equations, x_i is the mole fraction of component i , D_{ij} is the binary molecular-diffusion coefficient, $D_{\text{Kn},i}$ is the Knudsen diffusivity of component i , ϵ is the porosity of the support, p_i is the partial pressure of component i , and $J_{\text{md},i}$ is the flux of component i due to bulk and Knudsen diffusion. The binary molecular diffusion coefficient is calculated using the correlation of Fuller et al.,²⁸

$$D_{ij} = \frac{T^{1.75} \left(\frac{1}{\text{MW}_i} + \frac{1}{\text{MW}_j} \right)^{1/2}}{p \left[\left(\sum_i v_a \right)^{1/3} + \left(\sum_j v_a \right)^{1/3} \right]^2} \quad (14)$$

where MW_{*i*} is the molecular weight of component i , p is the total pressure, T is the temperature (K), and v_a are diffusion

volumes given by Fuller et al.²⁸ The Knudsen diffusivity is estimated from kinetic gas theory²

$$D_{\text{Kn},i} = \frac{\epsilon d_{\text{pore}}}{3} \left(\frac{8RT}{\pi M W_i} \right)^{1/2} \quad (15)$$

where the support pores are assumed to be cylindrical with a diameter of d_{pore} . Viscous flow, caused by finite pressure gradients across the pores, also contributes to the flow through the support² and is described by

$$J_{\text{visc},i} = - \left(\frac{P_i}{RT} \right) \frac{B}{\eta} \nabla p \quad (16)$$

where $J_{\text{visc},i}$ is the viscous contribution to the total flux through the support, η is the viscosity of the mixture, and B is the permeability of the support, given by

$$B = \frac{1}{\tau} \frac{d_{\text{pore}}^2}{32} \quad (17)$$

where τ is the tortuosity of the support. The total flux through the support is the sum of the two contributions

$$J_{s,i} = J_{\text{md},i} + J_{\text{visc},i} \quad (18)$$

and the transient flow is described by

$$\frac{\partial p_i}{\partial t} = -RT \frac{\partial J_{s,i}}{\partial z} \quad (19)$$

The support is on the permeate side of the zeolite, and the boundary conditions are the feed coverages given in eq 9 and the partial pressures in the permeate stream. The support model merges with the zeolite model at the zeolite/support interface, where equilibrium is assumed between the partial pressures in the support and the zeolite occupancies at the interface.

Athena Visual Workbench (www.athenavisual.com) was used to numerically integrate the partial differential equations by means of finite difference methods with a specified number of intervals in both the time and space domains. If the permeate partial pressures were not known, the model was run iteratively to determine them for a known total permeate pressure. The steady-state permeate mole fractions were calculated from the steady-state fluxes:

$$x_{i,\text{perm}} = \frac{J_{i,\text{SS}}}{J_{1,\text{SS}} + J_{2,\text{SS}}} \quad (20)$$

Results and Discussion

Transient permeation through a zeolite membrane was modeled for binary mixtures as a function of the ratios of single-component diffusivities and adsorption constants. The effects of the feed occupancy at steady state and the fractional occupancy of each component on the feed side were studied. Note that these fractional occupancies are functions of the feed pressures (or feed fugacities for liquids or high pressures) and the adsorption equilibrium constants. However, as shown below, for negligible support resistance and zero permeate pressure, the occupancy profiles and transient permeate behavior depend only on the feed occupancy, even though the feed occupancies were obtained by different combinations of feed pressures and adsorption equilibrium constants.

The same qualitative behavior presented here applies for given ratios of single-component diffusivities and feed occupancies,

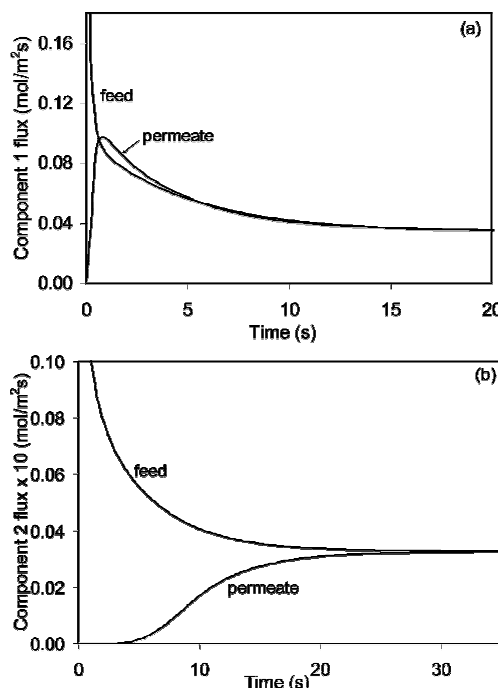


Figure 1. Transient response to a step increase in feed concentration to an empty zeolite membrane with negligible support resistance. Feed and permeate fluxes as a function of time for (a) faster-diffusing component 1 and (b) slower-diffusing component 2: $\Theta_1 = 5 \times 10^{-9} \text{ m}^2/\text{s}$, $\Theta_2 = 1 \times 10^{-10} \text{ m}^2/\text{s}$, $q_1^{\text{sat}} = q_2^{\text{sat}} = 2 \text{ mol/kg}$, $\delta = 100 \mu\text{m}$, $\rho = 1800 \text{ kg/m}^3$, $\theta_{1,\text{feed}} = \theta_{2,\text{feed}} = 0.33$, $\theta_{1,\text{perm}} = \theta_{2,\text{perm}} = 0$.

regardless of the values of the diffusivities, membrane thickness, saturation loadings, and zeolite density. For different parameter values, the time scale and magnitudes of the fluxes can be compared on the basis of the dimensionless quantities $(J_i \delta / \rho q_i^{\text{sat}} \Theta_i)$ and $(t \Theta_i / \delta^2)$. Thus, for the same feed occupancies and ratio of single-component diffusivities, increasing the membrane thickness by a factor of 10 decreases the steady-state flux by a factor of 10 and increases the time scale by a factor of 100 for the transient measurements, but the qualitative behavior does not change. If both single-component diffusivities and the membrane thickness were increased by a factor of 10, the flux does not change, and the time scale increases by a factor of 10 while the qualitative behavior is the same. For these calculations, Θ_1 was varied relative to a constant Θ_2 , but the qualitative behavior is the same regardless of which single-component diffusivity is held constant.

Diffusivities. Transient permeation of a binary mixture through an initially empty membrane was modeled for a zero permeate pressure and negligible support resistance. To determine how diffusivity differences influence transient behavior for the calculations in this section, the adsorption equilibrium constants and saturation loadings were the same for both components and $\Theta_1 = 50\Theta_2$. For most calculations in this section, the total fractional occupancy on the feed side was 0.67, and the feed mixture was equimolar. The feed fluxes at $t = 0$ are not included in the figures because the feed partial pressure was assumed to increase instantaneously, and thus, the occupancy gradient was initially infinite.

The transient behavior of the faster-diffusing component (Figure 1a) is qualitatively different from that for a single component, whereas the slower-diffusing component 2 (Figure 1b) exhibits behavior similar to that for a single component. The transient feed flux for a single component decreases and the permeate flux increases monotonically to steady state.^{15,16} In Figure 1a, the feed flux of the faster-diffusing component 1

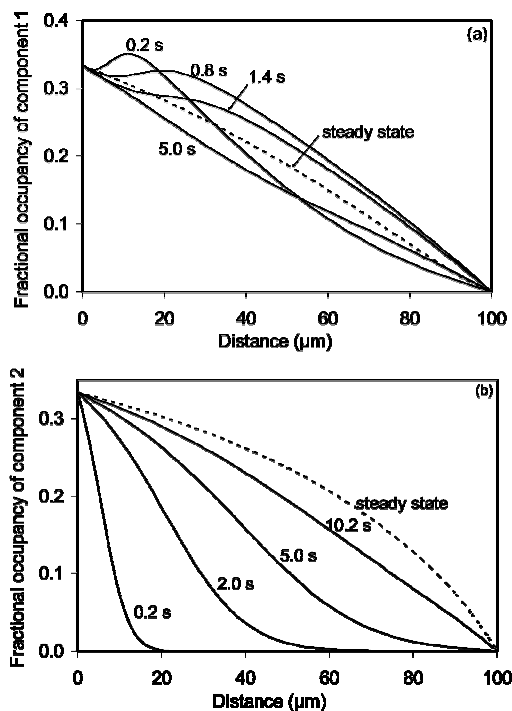


Figure 2. Transient response to a step increase in feed concentration to an empty zeolite membrane with negligible support resistance. Occupancy profiles for (a) faster-diffusing component 1 and (b) slower-diffusing component 2: $\bar{D}_1 = 5 \times 10^{-9} \text{ m}^2/\text{s}$, $\bar{D}_2 = 1 \times 10^{-10} \text{ m}^2/\text{s}$, $q_1^{\text{sat}} = q_2^{\text{sat}} = 2 \text{ mol/kg}$, $\delta = 100 \mu\text{m}$, $\rho = 1800 \text{ kg/m}^3$, $\theta_{1,\text{feed}} = \theta_{2,\text{feed}} = 0.33$, $\theta_{1,\text{perm}} = \theta_{2,\text{perm}} = 0$.

decreases to the steady-state flux monotonically, but its permeate flux exhibits a maximum before decreasing to the steady-state flux. Its permeate flux overshoots both the steady-state flux and the feed flux. The feed flux of the slower-diffusing component (Figure 1b) decreases and the permeate flux increases with time until they equal the steady-state flux. Note that the flux of component 2 was multiplied by 10 in Figure 1b to make the comparison of the fluxes of the two components easier. Note also that the time scales are different for parts a and b of Figure 1.

The faster-diffusing component 1 enters the membrane much quicker than the slower-diffusing component 2. The component 1 permeate flux increases rapidly initially, while component 2 permeate flux remains essentially zero. The component 1 permeate flux increases above what would be expected for a single component in the absence of component 2 because of the steep occupancy gradient of component 2. As component 2 diffuses into the membrane and displaces component 1, component 1 flux decreases. Component 2 slows the transport of component 1 once it enters the membrane, and this further contributes to the decrease in the component 1 flux. This type of behavior has been observed in both modeled and experimental systems.^{5,6,29} However, the behavior was attributed to the combined effects of the differences in adsorption and diffusion parameters. Krishna and Paschek⁵ stated that the maximum in the transient flux occurs for a fast-diffusing component with low adsorption strength when the feed also contains a slower-diffusing component with a higher adsorption strength. In Figure 1, a maximum occurs when the diffusivities are different but the adsorption strengths are the same; the maximum is not due to a difference in adsorption strengths in this case.

For the specific case shown in Figures 1 and 2, the flux 1/flux 2 ratio at steady state is ~ 10 , whereas the (\bar{D}_1/\bar{D}_2) ratio is 50. The flux ratio for single components is 50, but component 1

flux is lower in the mixture and component 2 flux is higher. That is, the slower-diffusing species (2) slows the faster-diffusing species (1) and vice versa.^{5,30,31} Additionally, the slower-diffusing species lowers the steady-state occupancy profile of the faster-diffusing species, and the faster-diffusing species raises the profile of the slower-diffusing species relative to the steady-state profile when both components have identical diffusivities. The steady-state occupancy profile of the faster-diffusing species is nearly linear, whereas the profile of the slower-diffusing species is highly nonlinear (Figure 2 parts a and b), even though the two species have the same feed occupancy.

The transient occupancy profiles (Figure 2 parts a and b) are consistent with the fluxes in Figure 1. The occupancy profiles of the faster-diffusing component 1 are markedly different (Figure 2a) from single-component profiles.^{15,16} For a single component diffusing through an initially empty membrane, the occupancy at any point in the membrane increases monotonically from zero to its steady state value. In Figure 2a, the occupancy, initially zero, increases at short times above the steady-state occupancy and exhibits a maximum near the feed side. This maximum propagates with time toward the permeate side. The component 1 occupancies decrease until they are less than the steady values almost everywhere in the membrane. The occupancies of component 1 then increase again to steady state. Occupancy profiles and their transient behavior for the slower-diffusing component 2 closely resemble those for the single component. The occupancy, initially zero, slowly increases from the feed side until it reaches steady state (Figure 2b). At steady state, the average time for a molecule to move through the membrane, calculated from the amount adsorbed at steady state divided by the steady-state flux, is approximately 2 s for component 1 and 23 s for component 2. The occupancies of each component are nonzero at the permeate side at much shorter times (less than 2 and 23 s) during the transient because the occupancy gradients are significantly greater during the transient than at steady state. The corresponding times for pure components at the same feed occupancies are 0.9 s for the faster and 44 s for the slower component.

At short times, component 1 flows from the feed to the permeate side, against its concentration gradient near the feed side (Figure 2a), because its flow is coupled to the flow of component 2, which has a large concentration gradient (Figure 2b). The faster-diffusing component 1 is pulled against its concentration gradient by the slower component, despite the relatively small amount of the slower component in the membrane. The chemical potential profiles (Figure 3 parts a and b), calculated from eq 2, show that the driving force is always in the direction of flow. The chemical potential of each component in Figure 3 was set equal to zero at the feed side. The chemical potentials at the permeate side are not identical in Figure 3b because a small, nonzero occupancy was assumed for numerical stability.

The maximum in component 1 occupancy profiles occurs slightly before the occupancy of the slower-diffusing component 2 becomes negligibly small (Figure 2). On the feed side of the maximum, the membrane contains significant amounts of both components, whereas on the permeate side of the maximum, the membrane contains primarily component 1. As the component 2 occupancy decreases across the membrane and its occupancy gradient becomes correspondingly lower, the overall driving force for component 1 decreases and shows a minimum at approximately the same location as the maximum in the

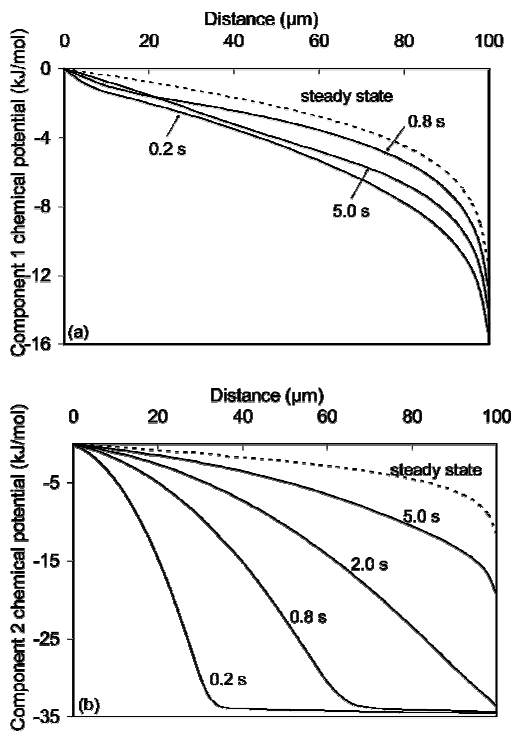


Figure 3. Transient response to a step increase in feed concentration to an empty zeolite membrane with negligible support resistance. Chemical potential profiles for (a) faster-diffusing component 1 and (b) slower-diffusing component 2. The chemical potential of each component was assigned a value of zero at the feed side: $\bar{D}_1 = 5 \times 10^{-9} \text{ m}^2/\text{s}$, $\bar{D}_2 = 1 \times 10^{-10} \text{ m}^2/\text{s}$, $q_1^{\text{sat}} = q_2^{\text{sat}} = 2 \text{ mol/kg}$, $\delta = 100 \mu\text{m}$, $\rho = 1800 \text{ kg/m}^3$, $\theta_{1,\text{feed}} = \theta_{2,\text{feed}} = 0.33$, $\theta_{1,\text{perm}} = \theta_{2,\text{perm}} = 0$.

occupancy. This can be seen in the inflection points in the component 1 chemical potential at short times (Figure 3a).

As $\bar{D}_{12} \rightarrow \infty$, the first term on the right-hand side of eq 1 goes to zero, and the effects of the exchange coefficient vanish. This is called the facile exchange scenario.¹¹ The equations for the fluxes are still coupled (eq 1), and the flux of the faster-diffusing component 1 still overshoots its steady-state value and increases above the feed flux (Figure 4a). Thus, the overshoot is due to the coupling of the fluxes rather than the effects of the exchange coefficient, but it is amplified by nonfacile exchange. The exchange coefficient represents the sorbate–sorbate interactions that lead to the faster component speeding up the slower and vice versa.^{5,30} When $\bar{D}_{12} \rightarrow \infty$, the steady-state occupancy profiles of both components are the same, they have the same shape as the single-component profile with a feed coverage of 0.66, and the steady-state flux of each component is half of its single-component flux at the total feed coverage. Thus, when $\bar{D}_{12} \rightarrow \infty$, permeation of each component is affected by the presence of the other component but is no longer affected by the diffusivity of the other component. Neither component is sped up or slowed by the other component, so both the ratio of the steady-state fluxes and the (\bar{D}_1/\bar{D}_2) ratio are 50. Both the maximum in the permeate flux and the steady-state flux of the faster-diffusing component are higher for infinite \bar{D}_{12} (Figure 4a) than for finite \bar{D}_{12} (Figure 1a), because the faster-diffusing component is not slowed by the slower-diffusing component when $\bar{D}_{12} \rightarrow \infty$. When sorbate–sorbate interactions are considered (finite \bar{D}_{12}), the faster component is slowed relatively more at steady state than during the transient because not much of the slower-diffusing component is in the membrane at short times during the transient. Thus, the increase of the maximum in the permeate flux during the transient for infinite \bar{D}_{12} over the maximum for finite \bar{D}_{12} is small relative to the

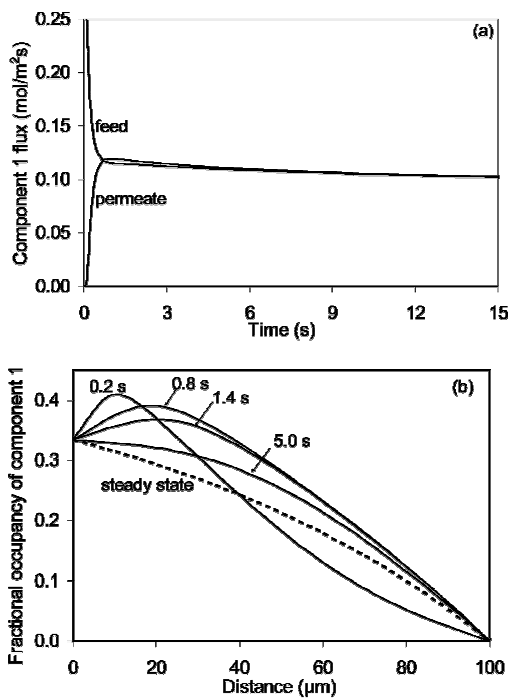


Figure 4. Transient response to a step increase in feed concentration to an empty zeolite membrane with negligible support resistance for $\bar{D}_{12} = \infty$. (a) Feed and permeate fluxes as a function of time and (b) transient occupancy profiles for the faster-diffusing component 1: $\bar{D}_1 = 5 \times 10^{-9} \text{ m}^2/\text{s}$, $\bar{D}_2 = 1 \times 10^{-10} \text{ m}^2/\text{s}$, $q_1^{\text{sat}} = q_2^{\text{sat}} = 2 \text{ mol/kg}$, $\delta = 100 \mu\text{m}$, $\rho = 1800 \text{ kg/m}^3$, $\theta_{1,\text{feed}} = \theta_{2,\text{feed}} = 0.33$, $\theta_{1,\text{perm}} = \theta_{2,\text{perm}} = 0$.

increase of the steady-state flux for infinite \bar{D}_{12} over the steady-state flux for finite \bar{D}_{12} , leading to a lower overshoot. Similarly, the maxima in the occupancy profiles of the faster-diffusing component (Figure 4b) are higher than those for a finite exchange coefficient (Figure 2a), because eliminating the exchange coefficient enhances the differences in the diffusion rates of the two components. Unlike Figure 2a, once the component 1 occupancy exceeds its steady-state value, it does not drop below steady state.

Feed and permeate responses were also calculated (with finite \bar{D}_{12}) for several ratios of diffusivities and for several feed occupancies. The maximum in the component 1 permeate flux (Figure 5) increases, relative to the steady-state flux, as both the feed occupancy and the ratio of the single-component M–S diffusivities increase. When the ratio of single-component diffusivities is 50, the overshoot increases from 20% of the steady-state flux at a total feed occupancy of 0.10 to 250% of steady state when the total feed occupancy is 0.95. At a total feed occupancy of 0.95 (Figure 5c), the overshoot increases from 11% of steady state when the ratio of single-component diffusivities is 2 to 250% of steady state when the diffusivity ratio is 50. For a given total feed occupancy, as (\bar{D}_1/\bar{D}_2) increases, more of the faster-diffusing component enters the membrane ahead of the slower component. The flux and occupancy of the faster-diffusing component reach higher values before the faster component is displaced by the slower-diffusing component. As the diffusivities become more different, the slower component slows the faster-diffusing component relatively more, and this further decreases the steady-state flux and increases the overshoot. As the total feed occupancy increases for a given (\bar{D}_1/\bar{D}_2) ratio, more of the faster component is available to enter the membrane and, correspondingly, more of the slower component is present to displace and slow it, and this leads to higher relative overshoots and maxima in the occupancy profiles. The overshoot is only ~0.1% when the total

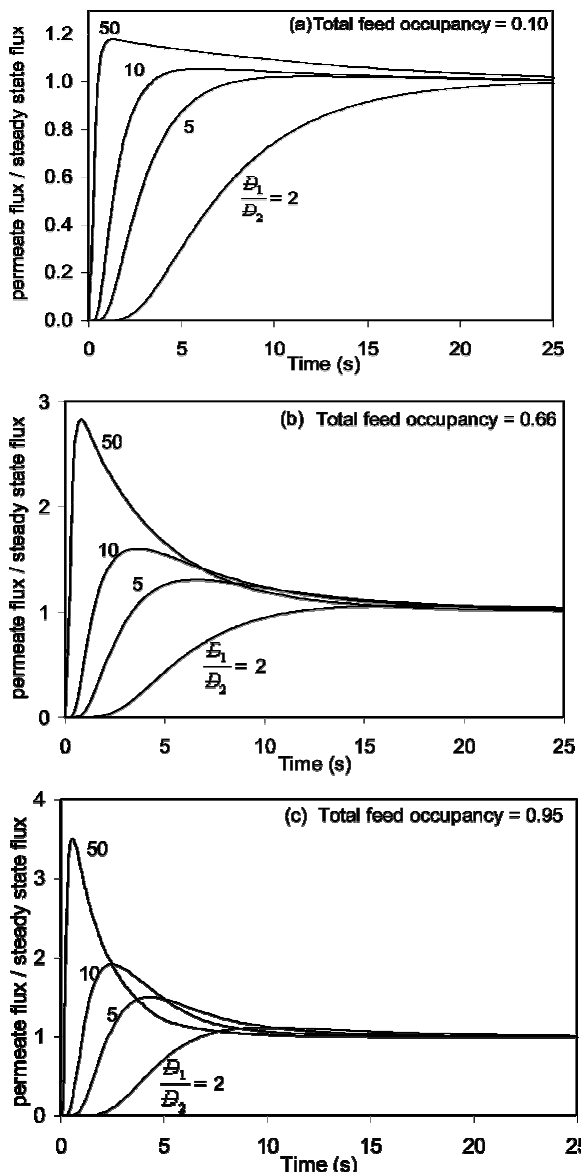


Figure 5. Transient permeate responses to a step increase in feed concentration to an empty zeolite membrane with negligible support resistance for ratios of $(\bar{D}_1/\bar{D}_2) = 2, 5, 10$, and 50 and total feed occupancies of (a) 0.10, (b) 0.66, and (c) 0.95: $\bar{D}_2 = 1 \times 10^{-10} \text{ m}^2/\text{s}$, $q_1^{\text{sat}} = q_2^{\text{sat}} = 2 \text{ mol/kg}$, $\delta = 100 \mu\text{m}$, $\rho = 1800 \text{ kg/m}^3$, $\theta_{1,\text{feed}} = \theta_{2,\text{feed}}$, $\theta_{1,\text{perm}} = \theta_{2,\text{perm}} = 0$.

Table 1. Steady-State Fluxes for Component 1 with Negligible Support Resistance as a Function of (\bar{D}_1/\bar{D}_2) and Total Feed Occupancy^a

(\bar{D}_1/\bar{D}_2)	component 1 steady-state flux $\times 10^2$ ($\text{mol/m}^2/\text{s}$)		
	total feed occupancy = 0.10	total feed occupancy = 0.66	total feed occupancy = 0.95
2	0.03	0.35	0.92
5	0.08	0.72	1.7
10	0.16	1.2	2.7
50	0.72	3.4	7.1

^a $\bar{D}_2 = 1 \times 10^{-10} \text{ m}^2/\text{s}$, $q_1^{\text{sat}} = q_2^{\text{sat}} = 2 \text{ mol/kg}$, $\delta = 100 \mu\text{m}$, $\rho = 1800 \text{ kg/m}^3$, $\theta_{1,\text{feed}} = \theta_{2,\text{feed}}$, $\theta_{1,\text{perm}} = \theta_{2,\text{perm}} = 0$.

feed occupancy is 0.10 and the (\bar{D}_1/\bar{D}_2) ratio is either 2 or 5. The steady-state fluxes for the curves in Figure 5 are given in Table 1.

For these calculations, the transients were modeled by increasing the feed occupancy instantaneously (a step function). For some conditions, the feed occupancies were ramped to the

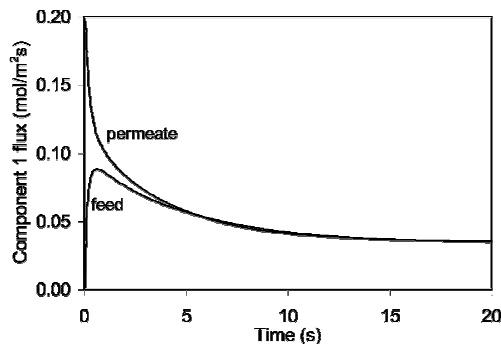


Figure 6. Transient response to a step change in feed composition to a zeolite membrane initially containing one of the two components at steady state and negligible support resistance. Feed and permeate fluxes as a function of time for the faster-diffusing component 1: $\bar{D}_1 = 5 \times 10^{-9} \text{ m}^2/\text{s}$, $\bar{D}_2 = 1 \times 10^{-10} \text{ m}^2/\text{s}$, $q_1^{\text{sat}} = q_2^{\text{sat}} = 2 \text{ mol/kg}$, $\delta = 100 \mu\text{m}$, $\rho = 1800 \text{ kg/m}^3$, $\theta_{1,\text{feed}} = \theta_{2,\text{feed}} = 0.33$, $\theta_{1,\text{perm}} = \theta_{2,\text{perm}} = 0$. The membrane initially contained the faster-diffusing component 1 at a steady state defined by $\theta_{1,\text{feed}} = 0.66$, $\theta_{1,\text{perm}} = 0$.

desired values in 1 s, and the overshoot in the transient response of the faster-diffusing component only changed by at most 5% of the overshoot obtained when the occupancies were increased instantaneously. Even when the feed occupancies were ramped to their desired value in 10 s, the overshoot changed by only 15% of the overshoot obtained when the occupancies were increased instantaneously. The amplitudes of the maxima in the occupancy profiles decreased as the feed occupancy of the slower component increased more slowly.

Transient permeation of a binary mixture, starting from a membrane initially filled with one component at steady state, was also modeled for a zero permeate pressure and negligible support resistance. When the membrane is initially filled with the faster-diffusing component at steady state, the behavior of the slower-diffusing component is qualitatively the same as that for an empty membrane (Figure 1b), and neither transient permeate flux exhibits a maximum (Figure 6). When the membrane is initially empty, component 1 enters the membrane faster than component 2, so that, as component 2 begins diffusing through, a significant amount of component 1 is already in the pores. The slower-diffusing component 2 diffuses through a membrane already containing component 1 in both Figure 6 and Figure 1, and thus, its behavior is expected to be similar in both cases. The feed flux of the faster-diffusing component 1 (Figure 6) exhibits a maximum while the permeate flux decreases monotonically to steady state. The negative feed flux immediately after addition of the slower-diffusing component 2 results from the decreased feed partial pressure of component 1. The component 1 feed flux quickly becomes positive because it depends on the steep gradient of component 2 in the direction of flow, meaning that component 2 pushes component 1 near the feed side. The occupancy gradient of the slower-diffusing component 2 decreases, and component 2 slows component 1 after enough of component 2 has entered the membrane; this causes the flux of component 1 to also decrease and results in a maximum in the feed flux.

The transient permeate flux of the added component 1 in a membrane initially filled with the slower-diffusing component 2 at steady state also shows no unusual behavior (Figure 7a). The negative feed flux of component 2 after the addition of component 1 (Figure 7b) results from the decreased feed partial pressure of component 2. This feed flux takes significantly longer to become positive than that for Figure 6, because the faster-diffusing component 1 (the added component) enters the membrane quicker than the added slower component in Figure 6.

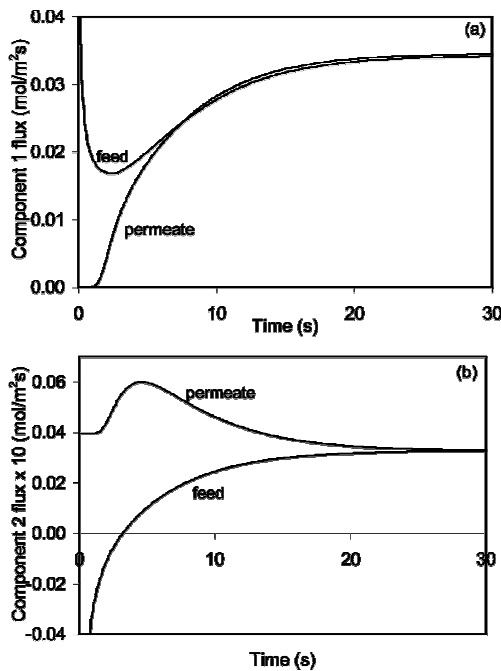


Figure 7. Transient response to a step change in feed composition to a zeolite membrane initially containing one of the two components at steady state and negligible support resistance. Feed and permeate fluxes as a function of time for (a) faster-diffusing component 1 and (b) slower-diffusing component 2: $\mathfrak{D}_1 = 5 \times 10^{-9} \text{ m}^2/\text{s}$, $\mathfrak{D}_2 = 1 \times 10^{-10} \text{ m}^2/\text{s}$, $q_1^{\text{sat}} = q_2^{\text{sat}} = 2 \text{ mol/kg}$, $\delta = 100 \mu\text{m}$, $\rho = 1800 \text{ kg/m}^3$, $\theta_{1,\text{feed}} = \theta_{2,\text{feed}} = 0.33$, $\theta_{1,\text{perm}} = \theta_{2,\text{perm}} = 0$. The membrane initially contained the slower-diffusing component 2 at a steady state defined by $\theta_{2,\text{feed}} = 0.66$, $\theta_{2,\text{perm}} = 0$.

6 and because the flux of component 2 out the feed side is slower than that of component 1 in Figure 6. Therefore, the occupancy gradient of the added component in Figure 7 is not as steep as that in Figure 6 shortly after the feed change, whereas the occupancy gradient of the original component in the opposite direction is higher in Figure 7 than in Figure 6. Thus, the driving force from permeate to feed side for component 2 in Figure 7 is present much longer than that for component 1 in Figure 6. The feed flux of the added, faster-diffusing component 1 goes through a minimum because it is affected by the backward diffusion of component 2. As this backward gradient decreases, the feed flux of component 1 begins to increase. The permeate flux of component 2 (Figure 7b) is briefly unaffected by the feed change, because the added component 1 has not yet reached the permeate side. This permeate flux then goes through a maximum as the slower-diffusing component 2 is pushed out of the membrane and sped up by the faster-diffusing component 1.

Adsorption Equilibrium Constants. The occupancy profile across a zeolite membrane with zero occupancy on the permeate side and negligible support resistance depends only on the diffusivity and the feed side occupancy. That is, the adsorption equilibrium constant only enters the permeance and the concentration profile calculations because it is used to determine the feed occupancy. Thus, the effect of different adsorption equilibrium constants for the two components was studied by varying the relative feed occupancies.

Transient permeation was modeled for an initially empty membrane, a permeate pressure of zero, and negligible support resistance. The two components had the same saturation loadings, and $\mathfrak{D}_1 = 50\mathfrak{D}_2$. The total feed occupancy was 0.95, with component 1 (the faster-diffusing species) having 26% of the total feed occupancy. For an equimolar feed mixture, this

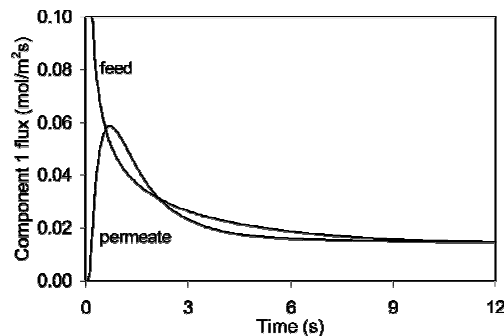


Figure 8. Transient response to a step increase in feed concentration to an empty zeolite membrane with negligible support resistance. Feed and permeate fluxes as a function of time for the faster-diffusing component: $\mathfrak{D}_1 = 5 \times 10^{-9} \text{ m}^2/\text{s}$, $\mathfrak{D}_2 = 1 \times 10^{-10} \text{ m}^2/\text{s}$, $q_1^{\text{sat}} = q_2^{\text{sat}} = 2 \text{ mol/kg}$, $\delta = 100 \mu\text{m}$, $\rho = 1800 \text{ kg/m}^3$, $\theta_{1,\text{feed}} = 0.25$, $\theta_{2,\text{feed}} = 0.70$, $\theta_{1,\text{perm}} = \theta_{2,\text{perm}} = 0$.

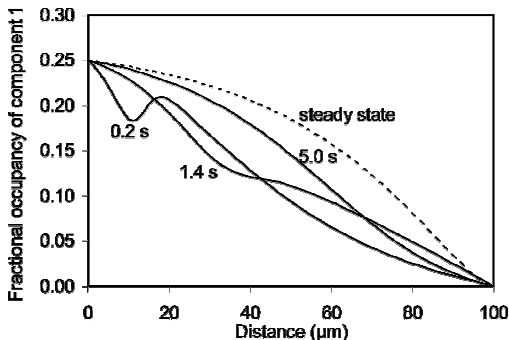


Figure 9. Transient response to a step increase in feed concentration to an empty zeolite membrane with negligible support resistance. Occupancy profiles for the faster-diffusing component 1: $\mathfrak{D}_1 = 5 \times 10^{-9} \text{ m}^2/\text{s}$, $\mathfrak{D}_2 = 1 \times 10^{-10} \text{ m}^2/\text{s}$, $q_1^{\text{sat}} = q_2^{\text{sat}} = 2 \text{ mol/kg}$, $\delta = 100 \mu\text{m}$, $\rho = 1800 \text{ kg/m}^3$, $\theta_{1,\text{feed}} = 0.25$, $\theta_{2,\text{feed}} = 0.70$, $\theta_{1,\text{perm}} = \theta_{2,\text{perm}} = 0$.

would correspond to the faster-diffusing component being more weakly adsorbed.

The transient behavior of the slower-diffusing component is analogous to that in Figure 1b. The transient behavior of the faster-diffusing component (Figure 8) is also similar to that in Figure 1a. However, the permeate flux, after overshooting the feed flux, decreases significantly below the feed flux. The overshoot in Figure 8 is 310% of the steady-state value, whereas the overshoot when the feed occupancies of both components are identical is 250%, even though the feed occupancy of component 1 is lower in Figure 8. The slower-diffusing component has a higher feed occupancy and, upon entering the membrane, slows and displaces the faster-diffusing component more than when the individual feed occupancies are identical. This pushes a wave of the faster-diffusing component through the membrane, decreases the steady-state flux, and amplifies the overshoot in the permeate flux.

The transient occupancy profiles of component 1 (Figure 9) correspond with the flux in Figure 8. The occupancy profiles of the slower-diffusing component are analogous to those in Figure 2b. The occupancy of the faster-diffusing component is initially zero, but at short times the profiles show both a local minimum and a local maximum, near the feed side; these move with time toward the permeate side. Unlike in Figure 2a, the occupancies never rise above the steady-state occupancies. As in Figure 2a, the occupancy gradient of component 1 is opposite the direction of flow for some regions of the membrane. Flow is from the feed to the permeate side because it is coupled with the occupancy gradient of component 2, and thus, component 1 is pushed against its concentration gradient by component 2.

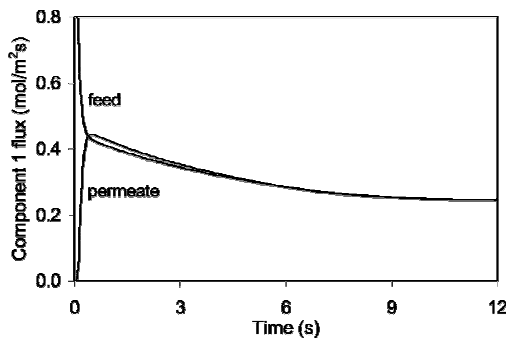


Figure 10. Transient response to a step increase in feed concentration to an empty zeolite membrane with negligible support resistance. Feed and permeate fluxes as a function of time for the faster-diffusing component: $D_1 = 5 \times 10^{-9} \text{ m}^2/\text{s}$, $D_2 = 1 \times 10^{-10} \text{ m}^2/\text{s}$, $q_1^{\text{sat}} = q_2^{\text{sat}} = 2 \text{ mol/kg}$, $\delta = 100 \mu\text{m}$, $\rho = 1800 \text{ kg/m}^3$, $\theta_{1,\text{feed}} = 0.70$, $\theta_{2,\text{feed}} = 0.25$, $\theta_{1,\text{perm}} = \theta_{2,\text{perm}} = 0$.

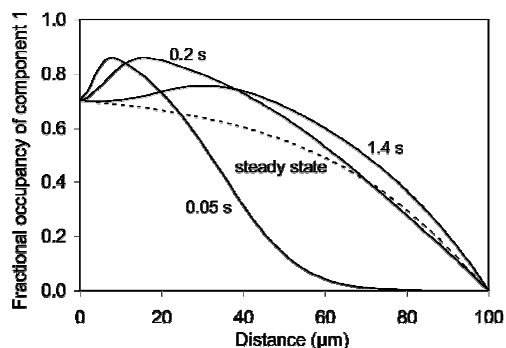


Figure 11. Transient response to a step increase in feed concentration to an empty zeolite membrane with negligible support resistance. Occupancy profiles for the faster-diffusing component 1: $D_1 = 5 \times 10^{-9} \text{ m}^2/\text{s}$, $D_2 = 1 \times 10^{-10} \text{ m}^2/\text{s}$, $q_1^{\text{sat}} = q_2^{\text{sat}} = 2 \text{ mol/kg}$, $\delta = 100 \mu\text{m}$, $\rho = 1800 \text{ kg/m}^3$, $\theta_{1,\text{feed}} = 0.70$, $\theta_{2,\text{feed}} = 0.25$, $\theta_{1,\text{perm}} = \theta_{2,\text{perm}} = 0$.

The chemical potential profiles calculated from eq 2 are consistent and show the driving force always in the direction of flow.

Simulations were also done where the total feed occupancy was 0.95, but the feed occupancy of the slower-diffusing component 2 was 26% of the total. For an equimolar feed mixture, this would correspond to the faster-diffusing component being more strongly adsorbed. The permeate flux of the faster-diffusing component (Figure 10) does not increase as far above the feed flux as it did in Figure 8, and it takes longer to decrease from the maximum than in Figure 8. The overshoot in Figure 10 is 80% of the steady-state value, less than that in Figure 8 because the feed occupancy of the slower-diffusing component is lower. The membrane contains less of the slower-diffusing component (because of its lower feed occupancy), so less of the faster-diffusing component is displaced, and the faster-diffusing component is not slowed as much, leading to a smaller overshoot. Consistent with the permeate flux, the occupancy profiles of the faster-diffusing component (Figure 11) rise above the steady-state profile but do not drop back below steady state as in Figure 2a, indicating that less of the faster-diffusing component is displaced.

The maximum in the permeate flux, relative to the steady-state flux, tends to increase as (a) the total occupancy increases, (b) the ratio of the single-component diffusivities increases, and (c) the fraction of the faster-diffusing component in the total feed occupancy decreases (Figure 12). However, when both the total feed occupancy and the ratio of the single-component diffusivities are high, the overshoot decreases slightly when the faster-diffusing component is a small fraction of the total feed occupancy (Figure 12 parts b and c). The overshoot increases

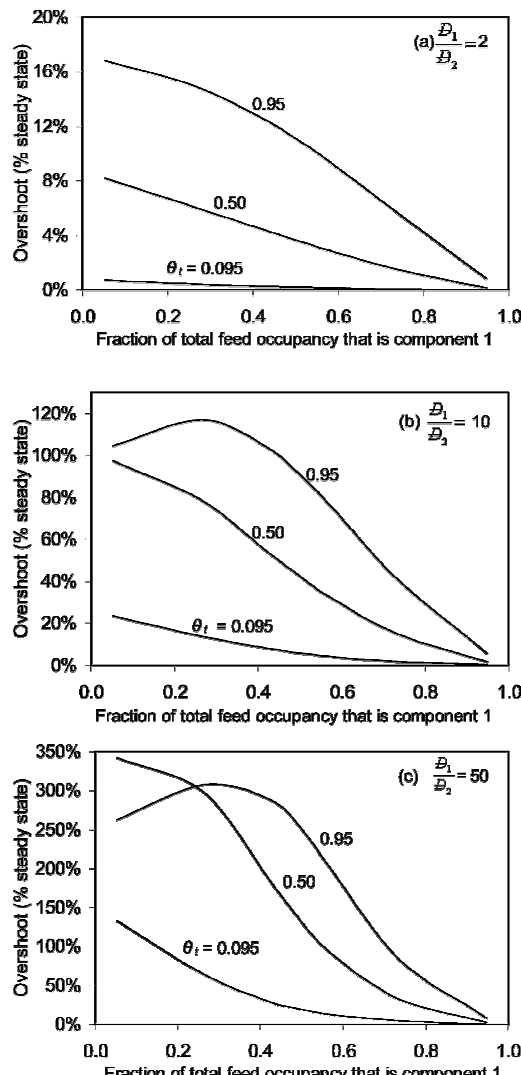


Figure 12. Overshoot (percentage of steady-state flux) in the permeate response of the faster-diffusing component to a step increase in feed concentration to an empty zeolite membrane with negligible support resistance for total feed occupancies of 0.095, 0.5, and 0.95 and (D_1/D_2) equal to (a) 2, (b) 10, and (c) 50: $D_2 = 1 \times 10^{-10} \text{ m}^2/\text{s}$, $q_1^{\text{sat}} = q_2^{\text{sat}} = 2 \text{ mol/kg}$, $\delta = 100 \mu\text{m}$, $\rho = 1800 \text{ kg/m}^3$, $\theta_{1,\text{perm}} = \theta_{2,\text{perm}} = 0$.

as the total occupancy and ratio of single-component diffusivities increase for the same reasons as for Figure 5. As the fraction of the faster-diffusing component in the total feed occupancy decreases for a given total feed occupancy and ratio of single-component diffusivities, more of the slower-diffusing component eventually enters the membrane, so the faster-diffusing component is displaced and slowed relatively more, leading to a higher overshoot. For an equimolar feed mixture, the relative overshoot is generally greater when the faster-diffusing component is more weakly adsorbed (has a lower fraction of the total feed occupancy).

Steady-State Occupancy Profiles. For single-component permeation with a permeate pressure of zero and negligible support resistance, the shape of the steady-state occupancy profile depends only on the feed occupancy. The profiles are highly nonlinear for high feed occupancies and approximately linear for low occupancies (Figure 13). Below a feed occupancy of ~ 0.30 , the normalized profiles are nearly linear. These occupancy profiles are identical, on a normalized-distance basis, independent of membrane thickness. Thus, for example, high feed occupancies are expected during pervaporation, and the

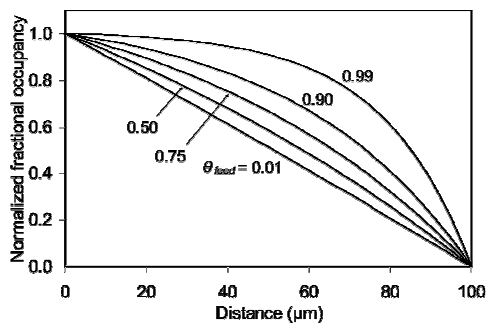


Figure 13. Single-component steady-state occupancy profiles in a $100\text{ }\mu\text{m}$ thick zeolite membrane with negligible support resistance and zero permeate pressure normalized by the feed occupancy for feed occupancies of 0.01, 0.50, 0.75, 0.90, and 0.99.

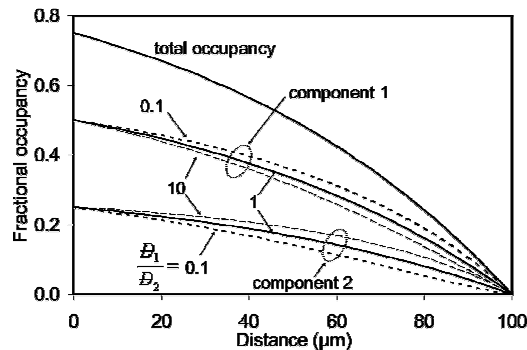


Figure 14. Steady-state occupancy profiles for a binary mixture in a $100\text{ }\mu\text{m}$ thick zeolite membrane with negligible support resistance and zero permeate pressure for a total feed occupancy of 0.75 and $(\mathfrak{D}_1/\mathfrak{D}_2) = 0.1, 1,$ and 10.

steady-state occupancy profiles will not be linear when the permeate pressure is zero and the support resistance can be neglected.

In two-component systems with a permeate pressure of zero and negligible support resistance, the steady-state occupancy profiles for each component depend only on the total feed occupancy, the individual component feed occupancies, and the ratio of the single-component diffusivities. The total occupancy profile is independent of the single-component diffusivities and is equivalent to the single-component profile (Figure 13) for the same total feed occupancy. When the single-component diffusivities are identical, the shapes of the individual-component occupancy profiles in the mixture (normalized by their respective feed occupancies) are identical to that of the total occupancy profile. When the single-component diffusivities are not the same, the shapes of the individual component occupancy profiles are not identical (Figure 14). An individual component occupancy profile is higher, relative to the profile when both diffusivities are equal, for the component with the lower diffusivity. Conversely, the profile of the component with the higher diffusivity is lower than that when both diffusivities are equal. The individual component profiles are also independent of membrane thickness when normalized.

Nonzero Permeate Pressure. Transient permeation of a binary mixture, starting from an empty membrane, was modeled for nonzero permeate pressures and negligible support resistance for two components with identical adsorption properties, but with $\mathfrak{D}_1 = 50\mathfrak{D}_2$. Figure 15 shows the behavior of the faster-diffusing component for different total permeate occupancies. As the total permeate occupancy increases from 0.05 to 0.4, the steady-state flux of the faster-diffusing component decreases from 95% to 44% of the steady-state flux obtained when the total permeate occupancy was zero (Table 2). The steady-state

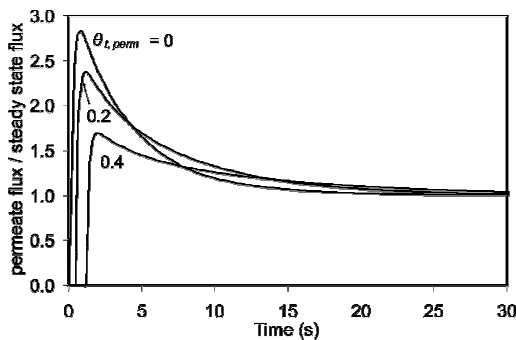


Figure 15. Transient permeate responses for the faster-diffusing component (normalized by the steady state) to a step increase in feed concentration to an empty zeolite membrane with negligible support resistance as a function of different total permeate occupancies: $\mathfrak{D}_1 = 5 \times 10^{-9}\text{ m}^2/\text{s}$, $\mathfrak{D}_2 = 1 \times 10^{-10}\text{ m}^2/\text{s}$, $q_1^{\text{sat}} = q_2^{\text{sat}} = 2\text{ mol/kg}$, $\delta = 100\text{ }\mu\text{m}$, $\rho = 1800\text{ kg/m}^3$, $\theta_{1,\text{feed}} = \theta_{2,\text{feed}} = 0.33$.

Table 2. Steady-State Fluxes and Permeate Occupancies as a Function of Total Permeate Occupancy for a Zeolite Membrane with Negligible Support Resistance^a

total permeate occupancy	steady-state flux $\times 10^2$ (mol/m ² /s)		permeate occupancies	
	(%) of steady-state flux when $\theta_{\text{perm}} = 0$)		component 1	component 2
	component 1	component 2		
0.05	3.3 (95%)	0.31 (95%)	0.045	0.005
0.10	3.1 (90%)	0.30 (90%)	0.09	0.01
0.20	2.7 (79%)	0.26 (80%)	0.18	0.02
0.30	2.2 (64%)	0.22 (68%)	0.27	0.03
0.40	1.5 (44%)	0.18 (56%)	0.36	0.04

^a $\mathfrak{D}_1 = 5 \times 10^{-9}\text{ m}^2/\text{s}$, $\mathfrak{D}_2 = 1 \times 10^{-10}\text{ m}^2/\text{s}$, $q_1^{\text{sat}} = q_2^{\text{sat}} = 2\text{ mol/kg}$, $\delta = 100\text{ }\mu\text{m}$, $\rho = 1800\text{ kg/m}^3$, $\theta_{1,\text{feed}} = \theta_{2,\text{feed}} = 0.33$.

flux of the slower-diffusing component decreases from 95% to 56% of the steady-state flux obtained when the permeate pressure was zero. The flux of the faster-diffusing component is affected more because its permeate occupancy increases proportionally more than that of the slower-diffusing component as the total permeate occupancy increases, because it has a higher concentration in the permeate stream (Table 2).

As the total permeate occupancy increases from 0.05 to 0.40, the overshoot in the permeate response of the faster-diffusing component decreases from 94% to 38% of the overshoot obtained when the total permeate occupancy was zero, because the driving force decreases as the permeate occupancy increases. A significant amount of the faster-diffusing component enters the membrane before the slower-diffusing component, even at high permeate pressure. The permeate occupancy of the faster-diffusing component increases as it reaches the permeate side, and thus, the driving force decreases and component 1 takes longer to reach the permeate side. For low permeate occupancy, the overshoot is high and the permeate response decreases quickly to steady state. As the permeate occupancy increases, the overshoot is smaller and the decrease to steady state takes longer (Figure 15).

Support Resistance. For composite membranes, as the pressure drop across the support increases, the pressure drop across the zeolite layer, and the permeate flux, decreases. Steady-state models containing contributions from combinations of molecular diffusion, Knudsen diffusion, and viscous flow have shown that the pressure drop across the support ranges from negligible to nearly the entire pressure drop across the system,³² depending on the operating conditions, support properties, and properties of the permeating components.^{32–35} For binary mixtures, the support has a larger effect on permeation of the

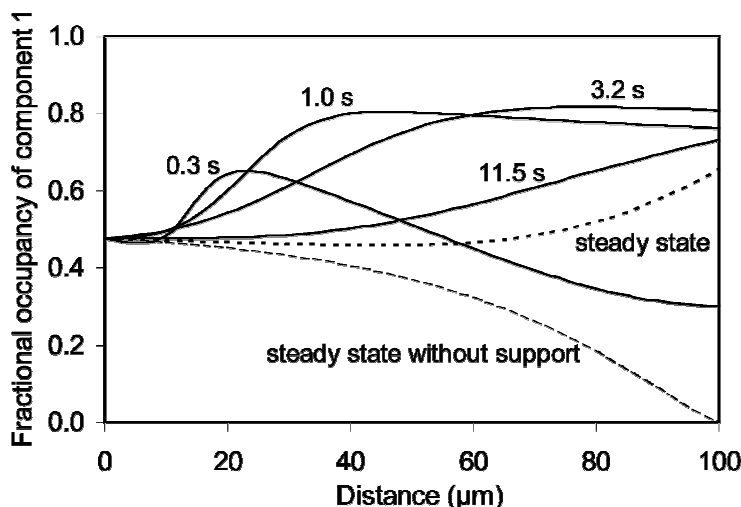


Figure 16. Transient response to a step increase in feed concentration to an empty zeolite membrane with zero permeate pressure. Occupancy profiles for the faster-diffusing component: $\bar{D}_1 = 5 \times 10^{-9} \text{ m}^2/\text{s}$, $\bar{D}_2 = 1 \times 10^{-10} \text{ m}^2/\text{s}$, $q_1^{\text{sat}} = q_2^{\text{sat}} = 2 \text{ mol/kg}$, $\delta = 100 \mu\text{m}$, $\delta_{\text{sup}} = 1 \text{ mm}$, $b_1 = b_2 = 1 \text{ kPa}^{-1}$, $\rho = 1800 \text{ kg/m}^3$, $\theta_{1,\text{feed}} = \theta_{2,\text{feed}} = 0.475$, $\theta_{1,\text{perm}} = \theta_{2,\text{perm}} = 0$, $\epsilon = 0.5$, $d_{\text{pore}} = 0.5 \mu\text{m}$, $\tau = 1.3$.

Table 3. Zeolite and Support Parameters

\bar{D}_1	$5 \times 10^{-9} \text{ m}^2/\text{s}$
\bar{D}_2	$1 \times 10^{-10} \text{ m}^2/\text{s}$
δ	$100 \mu\text{m}$
δ_{sup}	1 mm
$q_1^{\text{sat}} = q_2^{\text{sat}}$	2 mol/kg
ρ	1800 kg/m^3
$\theta_{1,\text{feed}} = \theta_{2,\text{feed}}$	0.475
$\theta_{1,\text{perm}} = \theta_{2,\text{perm}}$	0.0
τ	1.3
ϵ	0.5
d_{pore}	$0.5 \mu\text{m}$

more strongly adsorbing component.³³ Several studies examined the effects of both the support and sweep gas simultaneously,^{33–36} Skouidas and Sholl,³⁵ however, showed that, for CH₄ in silicalite at steady state, the support alone has a relatively minor effect on the permeate flux, whereas the effect of support and sweep gas combined can be more substantial.

In this study, the transient behavior was modeled, with a permeate pressure of zero and no sweep gas, for two components with the same adsorption equilibrium constant and saturation loading but different diffusivities. For a set feed occupancy from an equimolar feed mixture, the steady-state fluxes and the overshoot of the faster-diffusing component decrease as the strength of adsorption (equal for both components) or the support thickness increase. To keep the feed occupancies at the same value when the adsorption strengths were increased, the feed pressure was correspondingly decreased. The occupancies at the zeolite–support interface increase as the adsorption strengths increase or as the pressure drop across the support increases, and thus, the transmembrane gradients and fluxes decrease.

For the zeolite and support conditions in Table 3 and for $b = 1 \text{ kPa}^{-1}$, the overshoot in the permeate flux of the faster-diffusing component is 75% of the steady-state flux. The overshoot decreases approximately logarithmically from 145% to 19% as the adsorption equilibrium constant increases from 0.1 to 10 kPa⁻¹. The overshoot is lower at every point than when the support resistance was neglected. The overshoot results from the slower component both displacing some of the faster-diffusing component and also slowing it. Both components diffuse through the support at the same speed, and thus, the support dampens the overall difference in diffusion rates and decreases the overshoot. As the adsorption strength increases, the support enhances this dampening effect. Additionally, the

occupancy at the zeolite/support interface increases as the adsorption equilibrium constant increases, resulting in both a smaller driving force and a smaller overshoot in the permeate flux. For the conditions in Table 3 with $b = 1 \text{ kPa}^{-1}$, the overshoot increases from 61% to 84% of steady state as the porosity increases from 0.3 to 0.7, and it increases from 30% to 150% of steady state as the pore diameter increases from 0.1 to 5 μm . For the conditions in Table 3 and $b = 10 \text{ kPa}^{-1}$, the overshoot drops from 250% of the steady-state flux for no support to 19% for a 1 mm thick support. For a 5 mm support, the overshoot decreases to 11% of the steady-state flux. As the porosity decreases, the pore diameter decreases, or the support thickness increases, then the pressure drop across the support and the occupancy at the zeolite/support interface increase, which decreases the driving force and decreases the overshoot.

For the conditions in Table 3, the steady-state fluxes of both components are 88% ($b = 0.1 \text{ kPa}^{-1}$) and 16% ($b = 10 \text{ kPa}^{-1}$) of the fluxes without a support. The overshoot, relative to steady state, is 58% ($b = 0.1 \text{ kPa}^{-1}$) and 8% ($b = 10 \text{ kPa}^{-1}$) of the overshoot without support. The selectivity decreases from 99.7% ($b = 0.1 \text{ kPa}^{-1}$) to 65% ($b = 10 \text{ kPa}^{-1}$) of the selectivity without support. Thus, for strongly adsorbing components and thicker supports, the support significantly affects the steady-state flux, the selectivity, and the transient behavior. For more weakly adsorbed species and thinner supports, the support has more effect on transient behavior than on steady-state behavior. For example, for the conditions in Table 3, except with a 0.1 mm thick support and $b = 1 \text{ kPa}^{-1}$, the steady-state flux is nearly 90% and the selectivity is nearly 100% of that without the support, but the overshoot is <60% of that without the support.

The effect of the support on the occupancy profiles is shown in Figure 16 for the conditions in Table 3 with $b = 1 \text{ kPa}^{-1}$. The steady-state occupancy of the faster-diffusing component is higher at the permeate side than at the feed side (Figure 16). The partial pressure of this component is nearly a factor of 10 lower at the membrane/support interface than at the feed side, but the partial pressure of component 2 is low on the permeate side. Component 1 diffuses against its occupancy gradient, because the driving force results from the combined effects of the gradients of both components. As the feed occupancy decreases for given adsorption and support properties, the support affects both the steady-state and transient behavior more

Table 4. Steady-State Flux and Overshoot in the Permeate Flux of the Faster-Diffusing Component as a Function of Total Feed Occupancy in a Zeolite Membrane with Support Resistance^a

total feed occupancy	% of overshoot without support		% of flux without support	
	b = 0.1 kPa ⁻¹	b = 1 kPa ⁻¹	b = 0.1 kPa ⁻¹	b = 1 kPa ⁻¹
0.95	60	30	88	55
0.66	45	9	83	30

^a $\bar{D}_1 = 5 \times 10^{-9} \text{ m}^2/\text{s}$, $\bar{D}_2 = 1 \times 10^{-10} \text{ m}^2/\text{s}$, $q_1^{\text{sat}} = q_2^{\text{sat}} = 2 \text{ mol/kg}$, $\delta = 100 \mu\text{m}$, $\delta_{\text{sup}} = 1 \text{ mm}$, $\rho = 1800 \text{ kg/m}^3$, $\theta_{1,\text{feed}} = \theta_{2,\text{feed}}$, $\theta_{1,\text{perm}} = \theta_{2,\text{perm}}$ = 0, $\epsilon = 0.5$, $d_{\text{pore}} = 0.5 \mu\text{m}$, $\tau = 1.3$.

(Table 4); it accounts for a larger fraction of the pressure drop across the membrane so the overshoot and steady-state flux decrease.

Summary

(i) The permeate response of the faster-diffusing component in a binary mixture, during a transient response measurement in a zeolite membrane, overshoots the steady-state permeance even when adsorption properties of the two components are identical. The percent overshoot, in general, increases as the total feed occupancy increases, as the relative difference between the two single-component diffusivities increases, and as the fraction of the faster-diffusing component in the total feed occupancy decreases.

(ii) For zero permeate pressure and negligible support resistance, the adsorption equilibrium constant only affects the transient response by determining feed occupancies.

(iii) For single-component permeation with zero permeate pressure and negligible support resistance, the shape of the steady-state occupancy profile depends only on the feed occupancy. For binary mixtures with zero permeate pressure and negligible support resistance, the shape of the total occupancy profile depends only on the total feed occupancy. The individual component occupancy profiles depend only on the total feed occupancy, the individual feed occupancies, and the ratio of the single-component diffusivities.

(iv) As the total permeate occupancy increases, both the percent overshoot in the permeate response of the faster-diffusing component and steady-state flux of both components decrease. The total permeate occupancy has a larger effect on the steady-state behavior of the faster-diffusing component than on that of the slower-diffusing component.

(v) When the support resistance is not negligible, the support has a larger effect on the transient response than on the steady-state behavior of the more strongly adsorbing component for a given feed occupancy. The percent overshoot in the permeate response of the faster-diffusing component in a binary mixture decreases as the support porosity and support pore diameter decrease and the adsorption equilibrium constant and support thickness increase.

(vi) Transport can occur against the occupancy gradient of an individual component during both transient and steady-state permeation, because the chemical potential driving force results from the concentration gradients of both components.

Acknowledgment

We gratefully acknowledge support by the National Science Foundation, Grant CTS 0340563. We also thank Dr. Michael Caracotsios for his help with programming Athena Workshop.

Literature Cited

- (1) denExter, M. J.; Jansen, J. C.; vandeGraaf, J. M.; Kapteijn, F.; Moulijn, J. A.; vanBekkum, H. Zeolite-based membranes preparation, performance and prospects. *Recent Adv. New Horiz. Zeolite Sci. Technol.* **1996**, *102*, 413.
- (2) Krishna, R. A unified approach to the modelling of intraparticle diffusion in adsorption processes. *Gas Sep. Purif.* **1993**, *7*, 91.
- (3) Kapteijn, F.; Moulijn, J. A.; Krishna, R. The generalized Maxwell–Stefan model for diffusion in zeolites: sorbate molecules with different saturation loadings. *Chem. Eng. Sci.* **2000**, *55*, 2923.
- (4) Krishna, R.; Baur, R. Modelling issues in zeolite based separation processes. *Sep. Purif. Technol.* **2003**, *33*, 213.
- (5) Krishna, R.; Paschek, D. Separation of hydrocarbon mixtures using zeolite membranes: A modelling approach combining molecular simulations with the Maxwell–Stefan theory. *Sep. Purif. Technol.* **2000**, *21*, 111.
- (6) Krishna, R.; Vandenbroeke, L. J. P. The Maxwell–Stefan Description of Mass-Transport across Zeolite Membranes. *Chem. Eng. J.* **1995**, *57*, 155.
- (7) Bakker, W. J. W.; Kapteijn, F.; Poppe, J.; Moulijn, J. A. Permeation characteristics of a metal-supported silicalite-1 zeolite membrane. *J. Membr. Sci.* **1996**, *117*, 57.
- (8) Kapteijn, F.; Bakker, W. J. W.; Zheng, G.; Poppe, J.; Moulijn, J. A. Permeation and separation of light hydrocarbons through a silicalite-1 membrane—Application of the generalized Maxwell–Stefan equations. *Chem. Eng. J.* **1995**, *57*, 145.
- (9) van den Broeke, L. J. P. Ph.D. Thesis, Universiteit van Amsterdam, Amsterdam, The Netherlands, 1994.
- (10) Bakker, W. J. W.; Zheng, G.; Kapteijn, F.; Makkee, M.; Moulijn, J. A. Single and Multi-Component Transport through Metal-Supported MFI Zeolite Membranes. *Precis. Process. Technol.* **1993**, *425*.
- (11) Krishna, R.; Baur, R. Analytic solution of the Maxwell–Stefan equations for multicomponent permeation across a zeolite membrane. *Chem. Eng. J.* **2004**, *97*, 37.
- (12) Myers, A. L.; Prausnitz, J. M. Thermodynamics of Mixed-Gas Adsorption. *AIChE J.* **1965**, *11*, 121.
- (13) Krishna, R.; Smit, B.; Calero, S. Entropy effects during sorption of alkanes in zeolites. *Chem. Soc. Rev.* **2002**, *31*, 185.
- (14) Challa, S. R.; Sholl, D. S.; Johnson, J. K. Adsorption and separation of hydrogen isotopes in carbon nanotubes: Multicomponent grand canonical Monte Carlo simulations. *J. Chem. Phys.* **2002**, *116*, 814.
- (15) Gardner, T. Q.; Flores, A. I.; Noble, R. D.; Falconer, J. L. Transient Measurement of Adsorption and Diffusion in H-ZSM-5 Membranes. *AIChE J.* **2002**, *48*, 1155.
- (16) Gardner, T. Q.; Falconer, J. L.; Noble, R. D.; Zieverink, M. Analysis of Transient Permeation Fluxes into and out of Membranes for Adsorption Measurements. *Chem. Eng. Sci.* **2003**, *58*, 2103.
- (17) Gardner, T. Q.; Lee, J. B.; Noble, R. D.; Falconer, J. L. Adsorption and Diffusion Properties of Butanes in ZSM-5 Zeolite Membranes. *Ind. Eng. Chem. Res.* **2002**, *41*, 4094.
- (18) Gardner, T. Q.; Noble, R. D.; Falconer, J. L. Characterization of ZSM-5 and ZSM-11 Zeolite Membranes by Transient Permeation of Butanes. *AIChE J.* **2004**, *50*, 2816.
- (19) Bowen, T. C.; Wyss, J. C.; Noble, R. D.; Falconer, J. L. Measurements of diffusion through a zeolite membrane using isotopic-transient pervaporation. *Micropor. Mesopor. Mater.* **2004**, *71*, 199.
- (20) Bowen, T. C.; Wyss, J. C.; Noble, R. D.; Falconer, J. L. Inhibition during multicomponent diffusion through ZSM-5 zeolite. *Ind. Eng. Chem. Res.* **2004**, *43*, 2598.
- (21) Skouidas, A. I.; Sholl, D. S. Transport diffusivities of CH₄, CF₄, He, Ne, Ar, Xe, and SF₆ in silicalite from atomistic simulations. *J. Phys. Chem. B* **2002**, *106*, 5058.
- (22) Skouidas, A. I.; Sholl, D. S. Molecular dynamics simulations of self-diffusivities, corrected diffusivities, and transport diffusivities of light gases in four silica zeolites to assess influences of pore shape and connectivity. *J. Phys. Chem. A* **2003**, *107*, 10132.
- (23) Skouidas, A. I.; Sholl, D. S. Direct tests of the Darken approximation for molecular diffusion in zeolites using equilibrium molecular dynamics. *J. Phys. Chem. B* **2001**, *105*, 3151.
- (24) Krishna, R.; Paschek, D.; Baur, R. Modeling the occupancy dependence of diffusivities in zeolites. *Micropor. Mesopor. Mater.* **2004**, *76*, 233.
- (25) Krishna, R.; van Baten, J. M. Diffusion of alkane mixtures in zeolites: Validating the Maxwell–Stefan formulation using MD simulations. *J. Phys. Chem. B* **2005**, *109*, 6386.
- (26) Skouidas, A. I.; Sholl, D. S.; Krishna, R. Correlation effects in diffusion of CH₄/CF₄ mixtures in MFI zeolite. A study linking MD simulations with the Maxwell–Stefan formulation. *Langmuir* **2003**, *19*, 7977.

- (27) Chempath, S.; Krishna, R.; Snurr, R. Q. Nonequilibrium molecular dynamics simulations of diffusion of binary mixtures containing short *n*-alkanes in faujasite. *J. Phys. Chem. B* **2004**, *108*, 13481.
- (28) Fuller, E. N.; Schettler, P. D.; Giddings, J. C. A new method for the prediction of gas-phase diffusion coefficients. *Ind. Chem. Eng.* **1966**, *58*, 19.
- (29) Kapteijn, F.; Bakker, W. J. W.; Vandegraaf, J.; Zheng, G.; Poppe, J.; Moulijn, J. A. Permeation and Separation Behavior of a Silicalite-1 Membrane. *Catal. Today* **1995**, *25*, 213.
- (30) Krishna, R. Predicting transport diffusivities of binary mixtures in zeolites. *Chem. Phys. Lett.* **2002**, *355*, 483.
- (31) Sanborn, M. J.; Snurr, R. Q. Predicting membrane flux of CH₄ and CF₄ mixtures in faujasite from molecular simulations. *AIChE J.* **2001**, *47*, 2032.
- (32) de Bruijn, F. T.; Sun, L.; Olujic, Z.; Jansens, P. J.; Kapteijn, F. Influence of the support layer on the flux limitation in pervaporation. *J. Membr. Sci.* **2003**, *223*, 141.
- (33) Farooq, S.; Karimi, I. A. Modeling support resistance in zeolite membranes. *J. Membr. Sci.* **2001**, *186*, 109.
- (34) van de Graaf, J. M.; Kapteijn, F.; Moulijn, J. A. Methodological and operational aspects of permeation measurements on silicalite-1 membranes. *J. Membr. Sci.* **1998**, *144*, 87.
- (35) Skouidas, A. I.; Sholl, D. S. Multiscale models of sweep gas and porous support effects on zeolite membranes. *AIChE J.* **2005**, *51*, 867.
- (36) van de Graaf, J. M.; Kapteijn, F.; Moulijn, J. A. Modeling permeation of binary mixtures through zeolite membranes. *AIChE J.* **1999**, *45*, 497.

Received for review February 9, 2006
Revised manuscript received May 23, 2006
Accepted June 1, 2006

IE060166U